

# Gain without population inversion in V-type systems driven by a frequency-modulated field

Harshawardhan Wanare

*Department of Physics, Indian Institute of Technology, Kanpur 208016, Uttar Pradesh, India*  
(November 19, 2018)

We obtain gain of the probe field at multiple frequencies in a closed three-level V-type system using frequency modulated (FM) pump field. There is no associated population inversion among the atomic states of the probe transition. We describe both the steady-state and transient dynamics of this system. Under suitable conditions, the system exhibits large gain simultaneously at series of frequencies far removed from resonance. Moreover, the system can be tailored to exhibit multiple frequency regimes where the probe experiences anomalous dispersion accompanied by negligible gain-absorption over a large bandwidth, a desirable feature for obtaining superluminal propagation of pulses with negligible distortion.

42.50.Hz,42.50.Gy,32.80-t

## I. INTRODUCTION

In the last decade, a lot of remarkable effects of atomic coherence have been observed in various multilevel atoms [1]. One of these effects is lasing without inversion (LWI) [2] which has prospects in short-wavelength lasing. Conventional lasers based on population inversion become impractical in these wavelength regimes due to the  $\omega^3$  dependence of the Einstein A coefficient. Several experiments have provided unequivocal evidence of LWI; starting from amplification without inversion in transient [3] then in the steady state regime [4], leading ultimately to LWI [5]. In the LWI schemes an external driving field along a nearby transition generates atomic coherence which contributes to gain and alleviates the population inversion condition. In this paper we show another significant contribution that becomes operative in presence of strong modulation and results in gain at multiple frequencies. The conventional LWI based laser systems suffer from a major limitation due to the small gain they exhibit in comparison to the population inversion based laser systems. However, this difficulty is largely overcome in this FM field driven system because under suitable conditions one can obtain gain enhancement of ( $\sim 10^3\%$ ) with respect to the conventional LWI schemes (monochromatic field driven systems).

The FM field interacting with a two-level system has been intensely studied earlier [6–10] and more recently [11–15]. The FM pump field produces a large number of sidebands [13] which lead to periodic modulation of the absorption coefficient and the fluorescence signal [10]. Analytical solutions have been obtained for the weak modulation case in [8]. The periodic FM field forms the basis of ultrasensitive absorption spectroscopy [9,11] where the resonant information is made to ride on the modulation frequency or its harmonics thus overcoming the predominantly low frequency noise of lasers. The FM field provides many independent parameters which can be sensitively controlled and thus result in novel effects like the trapping of population [15], in multilevel systems suppression of a series of resonances occurs in the Autler-Townes spectra [16]. The trapping phenomenon due to the periodic FM field [17] or amplitude dependent phase modulation [20] can be exploited to achieve robust transfer of population across multiple levels. The systems driven by amplitude modulated field have also been widely studied: the two-level system [18] and the three-level system [19] both exhibit multiple resonances resulting from the modulation. We exploit the multiple resonances generated by the FM field and then tailor various parameters to obtain the desired gain features. To our knowledge studies have not been undertaken to obtain gain in multilevel systems using FM fields, particularly in the strong modulation regime, we undertake this study in this paper.

The organization of the paper is as follows: in section II we obtain the density matrix equations that govern the dynamics of the V-type system pumped by a FM field on one transition and is probed by a monochromatic field on the neighboring transition. We present the analysis of the results in section III, where we begin with the description of the steady state response of the system and go on to discuss the transient dynamics and finally discuss the physical basis of the gain obtained. In the steady state analysis we first deal with the off-resonant case where the central frequency of the FM field is detuned from atomic resonance followed by the on-resonance case. The contribution of atomic coherence between the two excited states of the V-type system is known to be responsible for inversionless probe gain in systems pumped by a monochromatic field [21,22]. Here, we describe another contribution which comes into being purely due to the modulation and plays a critical role in obtaining gain. We also describe the Floquet analysis which sheds light on the striking change that occurs in the probe spectrum at specific values of the index

of modulation. We utilize some of these features to obtain anomalous dispersion for the probe field accompanied by negligible absorption-gain in any desired frequency regime. This is an attractive feature for obtaining distortion free superluminal propagation [23]. Next, we describe the transient dynamics and try to identify the dominant nonlinear processes involved. The intricate dynamics of the time evolution is presented. We describe in detail the physical mechanism which is based on spontaneous emission assisted nonlinear optical process that we believe dominates the gain process. We present our conclusions in section IV.

## II. MODEL AND CALCULATION

We consider a closed three-level V-type system (Fig. 1) wherein, one of the transitions is coupled to a FM pump field and the other transition is coupled to a probe field as well as an incoherent (broadband) pump. The field at the atom is given as

$$\mathbf{E} = \mathbf{E}_1 e^{-i[\omega_1 t + \Phi(t)]} + \mathbf{E}_2 e^{-i\omega_2 t} + c.c.; \quad (1)$$

$$\Phi(t) = M \sin(\Omega t),$$

where  $\mathbf{E}_1$  ( $\mathbf{E}_2$ ) is the amplitude of the pump (probe) field, the FM field is sinusoidally modulated about the central frequency  $\omega_1$  and the modulation is characterized by two independent parameters - the frequency of modulation  $\Omega$  and the index of modulation  $M$ . The FM field couples the  $|1\rangle \leftrightarrow |3\rangle$  transition and the monochromatic probe field at  $\omega_2$  couples the  $|2\rangle \leftrightarrow |3\rangle$  transition.

The total Hamiltonian of the system is

$$H = \hbar\omega_{13}|1\rangle\langle 1| + \hbar\omega_{23}|2\rangle\langle 2| - \mathbf{d} \cdot \mathbf{E}, \quad (2)$$

where,  $\mathbf{d} = \mathbf{d}_{13}|1\rangle\langle 3| + \mathbf{d}_{23}|2\rangle\langle 3| + c.c.$  The first two terms in the Hamiltonian correspond to the unperturbed atomic system where the energies are measured from the ground state  $|3\rangle$ , and the last term is the interaction term in the dipole approximation. The semi-classical density matrix equation is

$$\frac{d\rho}{dt} = \frac{i}{\hbar}[H, \rho] - \gamma_1(|1\rangle\langle 1|\rho - 2\rho_{11}|3\rangle\langle 3| + \rho|1\rangle\langle 1|) - (\gamma_2 + \Lambda)(|2\rangle\langle 2|\rho - 2\rho_{22}|3\rangle\langle 3| + \rho|2\rangle\langle 2|) - \Lambda(|3\rangle\langle 3|\rho - 2\rho_{33}|2\rangle\langle 2| + \rho|3\rangle\langle 3|), \quad (3)$$

where,  $2\gamma_1$  ( $2\gamma_2$ ) is the rate of spontaneous emission from the level  $|1\rangle$  ( $|2\rangle$ ) to  $|3\rangle$ ,  $2\Lambda$  is the rate of incoherent pumping on the  $|2\rangle \leftrightarrow |3\rangle$  transition.

We transform the equation of motion (3) into a frame rotating with the instantaneous frequency of the field by using the following relations

$$\begin{aligned} \tilde{\rho}_{ii} &= \rho_{ii}, \quad i = 1, 2, 3, \\ \tilde{\rho}_{13} &= \rho_{13} e^{i[\omega_1 t + \Phi(t)]}, \\ \tilde{\rho}_{23} &= \rho_{23} e^{i\omega_2 t}, \\ \tilde{\rho}_{12} &= \rho_{12} e^{i[(\omega_1 - \omega_2)t + \Phi(t)]}, \end{aligned}$$

and undertake the rotating-wave approximation by neglecting the counter-rotating terms at nearly twice the optical frequency, like  $e^{\pm 2i[\omega_1 t + \Phi(t)]}$  and  $e^{\pm 2i\omega_2 t}$ . This approximation is valid if  $|d\Phi(t)/dt| \ll \omega_1$  which is valid for typical frequency modulation in the optical regime. Due to the coupling to the FM field the slowly varying density matrix ( $\tilde{\rho}$ ) equations involve time-dependent detuning factors which go as  $d\Phi(t)/dt$ .

We intend to obtain *exact* solutions of the density matrix equation for arbitrary strength of the fields and arbitrary values of the index of modulation. For this purpose we use the Fourier decomposition

$$\tilde{\rho}_{ij} = \sum_{n=-\infty}^{\infty} \rho_{ij}^{(n)} e^{-in\Omega t}; \quad i, j = 1, 2, 3, \quad (4)$$

which involves integral multiples of the frequency of modulation  $\Omega$ .

On substituting the expression (4) in the equation of evolutions of the slowly varying density matrix ( $\tilde{\rho}_{ij}$ ) and equating various powers of  $\Omega$ , we obtain the following infinite set of equations where  $n$  is an integer that varies from  $-\infty$  to  $\infty$ . The equations that govern the dynamics of the system are

$$\begin{aligned}
\frac{d\rho_{11}^{(n)}}{dt} &= -(2\gamma_1 - in\Omega)\rho_{11}^{(n)} + iG_1(\rho_{31}^{(n)} - \rho_{13}^{(n)}), \\
\frac{d\rho_{22}^{(n)}}{dt} &= -(2\gamma_2 + 2\Lambda - in\Omega)\rho_{22}^{(n)} + 2\Lambda\rho_{33}^{(n)} + iG_2(\rho_{32}^{(n)} - \rho_{23}^{(n)}), \\
\frac{d\rho_{33}^{(n)}}{dt} &= -(2\Lambda - in\Omega)\rho_{33}^{(n)} + (2\Lambda + 2\gamma_2)\rho_{22}^{(n)} + 2\gamma_1\rho_{11}^{(n)} - iG_1(\rho_{31}^{(n)} - \rho_{13}^{(n)}) - iG_2(\rho_{32}^{(n)} - \rho_{23}^{(n)}), \\
\frac{d\rho_{12}^{(n)}}{dt} &= -(\gamma_1 + \gamma_2 + \Lambda - i(\Delta_1 - \Delta_2) - in\Omega)\rho_{12}^{(n)} + iG_1\rho_{32}^{(n)} - iG_2\rho_{13}^{(n)} + \frac{iM\Omega}{2}(\rho_{12}^{(n+1)} + \rho_{12}^{(n-1)}), \\
\frac{d\rho_{13}^{(n)}}{dt} &= -(\gamma_1 + \Lambda - i\Delta_1 - in\Omega)\rho_{13}^{(n)} + iG_1(\rho_{33}^{(n)} - \rho_{11}^{(n)}) - iG_2\rho_{12}^{(n)} + \frac{iM\Omega}{2}(\rho_{13}^{(n+1)} + \rho_{13}^{(n-1)}), \\
\frac{d\rho_{23}^{(n)}}{dt} &= -(\gamma_2 + 2\Lambda - i\Delta_2 - in\Omega)\rho_{23}^{(n)} + iG_2(\rho_{33}^{(n)} - \rho_{22}^{(n)}) - iG_1\rho_{21}^{(n)},
\end{aligned} \tag{5}$$

where  $\Delta_1 = \omega_{13} - \omega_1$  is the detuning of the central frequency of the FM field from the atomic resonance on the  $|1\rangle \leftrightarrow |3\rangle$  transition, the probe field detuning is  $\Delta_2 = \omega_{23} - \omega_2$  on the  $|2\rangle \leftrightarrow |3\rangle$  transition. The strength of the atom-field coupling is given by the Rabi frequency  $2G_i = 2\mathbf{d}_{i3} \cdot \mathbf{E}_i/\hbar$  on the  $|i\rangle \leftrightarrow |3\rangle$  transition, for  $i = 1$  and  $2$  denoting the pump and probe Rabi frequencies, respectively. The six equations in Eqs. (5) and three equations of motion for  $\rho_{21}^{(n)}$ ,  $\rho_{31}^{(n)}$  and  $\rho_{32}^{(n)}$  form a set of nine equations for each  $n$ . We note that the set of equations for  $n$  are coupled to set for  $n \pm 1$ . The closure of the above system requires that  $\rho_{11}^{(n)} + \rho_{22}^{(n)} + \rho_{33}^{(n)} = \delta_{n,0}$ .

We obtain exact non-perturbative solutions of the above equations in both the transient as well as steady-state regimes. The transient solutions are obtained by taking a large set of closed  $(2N+1) \times 9$  first order coupled differential equations where the harmonic index  $n$  varies from  $-N$  to  $N$ , and numerically integrating them using fourth-order Runge-Kutta routine. Needless to say, we have checked the convergence of the solutions by increasing  $N$  and decreasing the step-size of integration. We obtain the steady-state solutions by setting the left hand side time derivatives to zero in Eqs. (5) and obtain tri-diagonal recurrence relations which are solved using the infinite continued fraction technique [24,10].

### III. RESULTS AND DISCUSSION

#### A. Steady-state response

We present the steady-state response of the system described in section II. We consider two different cases, first one is the off-resonant case wherein the central frequency of the FM field is detuned from the atomic transition ( $\Delta_1 \neq 0$ ), and the second case where the central frequency of the FM field is on resonance with the atomic transition. The second case permits a comparison with the usual system pumped by a monochromatic field instead of the FM field [21]. In all our calculations the relevant frequency/time variables are appropriately normalized with the spontaneous emission decay on the pump transition, namely  $\gamma_1$ .

In presence of the FM field on  $|1\rangle \leftrightarrow |3\rangle$  transition, the probe field on the  $|3\rangle \leftrightarrow |2\rangle$  transition exhibits two combs of absorption peaks which are slightly displaced from each other. Each comb has frequencies that are separated by  $\sim \pm\Omega$  and the relative shift between the combs depends on  $M$ ,  $\Delta_1$  and  $G_1$ . The overall spectrum appears as a series of double peak structures displaced by  $\sim \pm\Omega$ . The width of the resonances depend on the incoherent processes like the decays and the incoherent pump. Fig. 2a shows a typical absorption spectrum of the probe field modified by a strong FM field on the neighboring transition. In our notation, absorption of the probe field occurs when  $\text{Im}(\rho_{32}^{(0)}) < 0$ . The two displaced comb like resonances result from probing the two linearly independent set of Floquet states resulting from the time periodic nature of the FM field-atom interaction. We discuss these aspects in detail below.

In presence of the incoherent pump  $\Lambda$  one comb of frequencies experiences gain ( $\text{Im}(\rho_{32}^{(0)}) > 0$  corresponds to probe gain). The two set of combs continue to remain displaced and one of them is flipped over in the opposite direction exhibiting gain as seen in Fig. 2b.

In terms of the density matrix equations the steady state contributions to the probe gain/absorption can be resolved into three different terms, namely,

$$F_1 = \frac{i G_2 (\rho_{22}^{(0)} - \rho_{33}^{(0)}) (\gamma_1 + \gamma_2 + \Lambda - i(\Delta_1 - \Delta_2))}{(\gamma_1 + \gamma_2 + \Lambda - i(\Delta_1 - \Delta_2))(\gamma_2 + 2\Lambda + i\Delta_2) + G_1^2},$$

$$\begin{aligned}
F_2 &= \frac{G_2 G_1 \rho_{13}^{(0)}}{(\gamma_1 + \gamma_2 + \Lambda - i(\Delta_1 - \Delta_2))(\gamma_2 + 2\Lambda + i\Delta_2) + G_1^2}, \\
F_3 &= -\frac{M\Omega}{2} \times \frac{G_1 (\rho_{12}^{(1)} + \rho_{12}^{(-1)})}{(\gamma_1 + \gamma_2 + \Lambda - i(\Delta_1 - \Delta_2))(\gamma_2 + 2\Lambda + i\Delta_2) + G_1^2}, \\
\rho_{32}^{(0)} &= F_1 + F_2 + F_3.
\end{aligned} \tag{6}$$

The first term  $F_1$  contains the contribution of the population difference between the energy levels  $|2\rangle$  and  $|3\rangle$  (when  $M = 0$  it corresponds to the conventional population inversion term), the next two terms correspond to the coherence term in the conventional modulation free ( $M = 0$ ) scheme [21,22]. Note that all the three components have the same denominator. The second term  $F_2$  provides the probe response to the dynamics at the central FM frequency  $\omega_1$ , or, to the  $n = 0$  contribution on the  $|1\rangle \leftrightarrow |3\rangle$  transition. The third term  $F_3$ , we call the modulation term, provides the contributions arising purely due to modulation. The contributions from the higher order terms, namely  $|n| \geq 1$ , are mainly channeled through the  $F_3$  term. Note that the  $F_3$  term provides the coupling of  $n = 0$  response to the  $n = \pm 1$  term and this coupling is proportional to  $G_1 M \Omega$ , moreover, the coupling is independent of the probe Rabi frequency  $G_2$ . Similar expressions can be written for each  $n$  and the coupling from higher order terms  $n \pm 1$  always occurs through  $G_1 M \Omega$  and is independent of  $G_2$ . No approximations are made in writing out the various components in Eq. (6), all the individual factors contained therein, like  $\rho_{22}^{(0)}, \rho_{33}^{(0)}, \rho_{13}^{(0)}$  and  $\rho_{12}^{(\pm 1)}$ , are calculated exactly and thus contain all the higher order contributions.

The major contribution from the first two terms ( $F_1$  and  $F_2$ ) for a weak probe occur at frequencies

$$\Delta_2 \rightarrow \frac{\Delta_1}{2} \pm \frac{1}{2} \sqrt{\Delta_1^2 + 4G_1^2}, \tag{7}$$

which is similar to the usual monochromatic pump case. The third term  $F_3$  provides the higher order contributions which become significant in presence of strong modulation due to the coupling proportional to  $G_1 M \Omega$ , as seen in Eq. (6). For the parameters chosen for Fig. 2, the contribution from the  $F_3$  term dwarfs the  $F_1$  and  $F_2$  contributions at all the frequencies other than those given in Eq. (7), see Fig. 2c. Thus, in the strong modulation regime the modulation term dominates over the population inversion and the coherence terms of the usual monochromatic pump case.

In order to understand the two comb of resonances one can obtain the Floquet spectrum resulting from the FM field coupling the atomic transition. Moreover, it has been demonstrated that in presence of strong modulation and under certain conditions the Autler-Townes response exhibits simultaneous suppression of semi-infinite number of resonances [16]. The conditions under which this occurs can also be obtained by analyzing the Floquet-spectrum. Following the approach developed by Shirley [25] to obtain the Floquet states, we consider exactly the effect of the strong FM field on the atomic transition and neglect the weak effects of dissipation and the weak probe field because  $G_1, \Omega \gg \gamma_1, \gamma_2, \Lambda, G_2$ . In this limit it is advantageous to look at the dressed states  $|\Psi_1\rangle$  and  $|\Psi_3\rangle$  (dressed by the FM field) instead of the bare atomic states  $|1\rangle$  and  $|3\rangle$ . The Schrödinger equation of the evolution of the corresponding dressed state amplitudes  $\psi_1$  and  $\psi_3$  is

$$i \frac{d}{dt} \begin{pmatrix} \psi_1 \\ \psi_3 \end{pmatrix} = \begin{pmatrix} \Delta_1 - M\Omega \cos(\Omega t) & -G_1 \\ -G_1 & 0 \end{pmatrix} \begin{pmatrix} \psi_1 \\ \psi_3 \end{pmatrix}. \tag{8}$$

As the Hamiltonian in Eq. (8) depends on time periodically, with a period  $2\pi/\Omega$ , one can obtain two linearly independent solutions of Eq. (8) in the following form

$$\psi_i^\pm(t) = e^{-i\lambda_\pm t} \sum_{n=-\infty}^{\infty} \chi_i^{\pm, n} e^{-in\Omega t} \quad (i = 1 \text{ and } 3), \tag{9}$$

where the index  $+$  and  $-$  distinguish the two solutions. On substituting expression (9) into Eq. (8) we obtain an infinite set of recursion relations for  $\chi_i^n$ ,  $i = 1$  and  $3$

$$\begin{pmatrix} -n\Omega + \Delta_1 & -G_1 \\ -G_1 & -n\Omega \end{pmatrix} \begin{pmatrix} \chi_1^n \\ \chi_3^n \end{pmatrix} - \frac{M\Omega}{2} \begin{pmatrix} 1 & 0 \\ 0 & 0 \end{pmatrix} \left[ \begin{pmatrix} \chi_1^{n+1} \\ \chi_3^{n+1} \end{pmatrix} + \begin{pmatrix} \chi_1^{n-1} \\ \chi_3^{n-1} \end{pmatrix} \right] = \lambda \begin{pmatrix} \chi_1^n \\ \chi_3^n \end{pmatrix}, \tag{10}$$

wherein  $\chi_i^n$  is coupled to its nearest neighbors  $\chi_i^{n\pm 1}$ , for brevity we have dropped the  $\pm$  superscript. These recursion relations can be written as an infinite matrix eigenvalue problem with the following infinite dimensional Hamiltonian ( $H_f$ )

$$\begin{pmatrix} \dots & \vdots & \vdots & \vdots & \vdots & \vdots & \downarrow & \vdots & \vdots & \vdots & \dots \\ \dots & -\frac{M\Omega}{2} & 0 & -(n-1)\Omega + \Delta_1 & -G_1 & -\frac{M\Omega}{2} & 0 & 0 & 0 & 0 & \dots \\ \dots & 0 & 0 & -G_1 & -(n-1)\Omega & 0 & 0 & 0 & 0 & 0 & \dots \\ \dots & 0 & 0 & -\frac{M\Omega}{2} & 0 & -n\Omega + \Delta_1 & -G_1 & -\frac{M\Omega}{2} & 0 & 0 & \dots \\ \rightarrow & 0 & 0 & 0 & 0 & -G_1 & -n\Omega & 0 & 0 & 0 & \dots \\ \dots & 0 & 0 & 0 & 0 & -\frac{M\Omega}{2} & 0 & -(n+1)\Omega + \Delta_1 & -G_1 & -\frac{M\Omega}{2} & \dots \\ \dots & 0 & 0 & 0 & 0 & 0 & 0 & -G_1 & -(n+1)\Omega & 0 & \dots \\ \dots & \vdots & \vdots & \vdots & \vdots & \vdots & \vdots & \vdots & \vdots & \vdots & \dots \end{pmatrix}. \quad (11)$$

Here, we have ordered the elements of the Floquet Hamiltonian  $H_f$  such that  $i$  runs over the states 1 and 3 before a change in the harmonic index  $n$  which takes integer values from  $-\infty$  to  $\infty$ . The eigenvalues of the  $H_f$  matrix are the quasienergies associated with various levels of the dressed states. The structure of the matrix (11) results in periodic eigenvalues, and each dressed state has an infinite ladder of quasienergy levels separated by  $\pm\Omega$ . In other words the comb of resonances correspond to probing the two linearly independent set of dressed states  $+$  and  $-$ , whose energies given by  $\lambda_{\pm} + n\Omega$ , where  $n$  takes integer values from  $-\infty$  to  $\infty$ . Moreover, two levels belonging to different dressed states complement each other, i.e.,  $\lambda_+ - \lambda_- = \Delta_1$  modulo( $\Omega$ ).

It has been shown in detail [16] that when

$$\lambda + m\Omega = 0 \quad (12)$$

for some integer  $m$  the determinant of the characteristic equation of the above eigenvalue problem factorizes into determinants of two semi-infinite blocks

$$\det[H_f - \mathbf{I}\lambda]_{\lambda=-m\Omega} = -G_1^2 \det[H_a - \mathbf{I}\lambda] \det[H_b - \mathbf{I}\lambda] = 0. \quad (13)$$

The two semi-infinite blocks are such that the harmonic index  $n$  in  $H_a$  and  $H_b$  runs from  $-\infty$  to  $m-1$  and  $m+1$  to  $\infty$ , respectively. The quasienergies are ambiguous within integer multiple of  $\Omega$  because replacing  $\lambda$  by  $\lambda + k\Omega$ , where  $k$  is an integer, leaves the Eq. (13) unchanged. The above factorization results from the structure of the Floquet Hamiltonian - if the integer  $m$  happens to be  $n$  in matrix (11) then the row and column marked by small horizontal and vertical arrows, respectively, in the matrix Eq. (11) contains only one non-trivial element namely  $-G_1$ , corresponding to the  $\chi_3^m$  term. Now if  $\chi_3^m = 0$  then the half-infinite system of equations is closed resulting in the above factorization, eq. (13). To determine bounded non-trivial solutions of the characteristic equation (13) one requires that one of the following conditions is satisfied, either

$$\det[H_a + \mathbf{I} m\Omega] = 0 \quad \text{or} \quad \det[H_b + \mathbf{I} m\Omega] = 0. \quad (14)$$

The above conditions results in

$$\chi_1^n = \chi_3^n = 0 \quad \text{for all } n < m \quad \text{or} \quad n > m \quad (15)$$

depending on which of the conditions in Eq. (14) is satisfied. The various harmonics of the dressed states  $\chi_i^n$  and the corresponding quasienergies  $\lambda$  are determined numerically with the dimensions of the Floquet Hamiltonian matrix to be  $2(N+1)$  where  $N$  is a large positive integer and the harmonic index  $n$  in eq. (11) varies from  $-N$  to  $N$ .

We calculate the variation of the quasienergies as a function of the modulation index  $M$  for a fixed value of the pump field coupling strength, its detuning and the modulation frequency. In Fig. 3a the corresponding parameters are  $G_1 = 20\gamma_1$ ,  $\Delta_1 = 20\gamma_1$ , and  $\Omega = 30\gamma_1$ . Henceforth, we drop the harmonic superscript  $(o)$  from the density matrix variables as we will deal with only the zeroth order atomic response at the frequencies  $\omega_1$  and  $\omega_2$  unless otherwise specified. As seen in Fig. 3a, the quasienergy level plotted with a solid line crosses the zero energy periodically at  $M = 2.915, 4.06, 6.26, 7.35$  and so on. At these values of  $M$  the condition (12) is satisfied. The probe spectrum exhibits only one set of absorption peaks separated by  $\Omega$ , instead of the usual set of double peaks, as Eq. (15) is satisfied. Fig. 3b highlights this feature for  $M = 2.915$  which is the first zero crossing of the quasienergy level in Fig. 3a. There is only single peaked structure for  $\Delta_2 > 0$ , whereas the spectra for  $\Delta_2 < 0$  continues to exhibit the two set of peaks. In Fig. 3b the probe response is shown for various values of the incoherent pump  $\Lambda/\gamma_1 = 0, 0.2, 0.4, 0.6, 0.8$  and  $1.0$ . In the absence of the incoherent pump the probe absorption spectra for  $\Delta_2 < 0$  contains two comb of absorption dips, whereas for  $\Delta_2 > 0$  it contains a single comb of absorption dips separated by  $\sim \Omega$ . As the incoherent pump rate is increased one set of absorption dips transform into gain peaks. The gain is maximum at about  $\Lambda/\gamma_1 = 0.5$ . We have observed that for parameters where the semi-infinite resonances are suppressed, the surviving single comb of resonances almost always exhibit gain in presence of the incoherent pump.

As the probe spectrum shows well separated gain peaks (for  $\Delta_2 > 0$ ) the intermediate region accords the possibility of anomalous dispersion. In these frequency regimes the probe beam can experience superluminal velocity due to

anomalous dispersion [23]. Regions of anomalous dispersion ( $d \operatorname{Re}(\rho_{32})/d\omega_2 < 0$ ) accompanied by a flat region of nearly zero absorption ( $\operatorname{Im}(\rho_{32}) \approx 0$ ) is particularly desirable in achieving superluminal propagation. In Fig. 4, the region between a set of gain peaks is expanded and one can see the anomalous dispersion accompanied by a flat region of negligible gain/absorption. The superluminal propagation in Ref. [23] is achieved in between Raman gain lines. The anomalous region between the gain lines, in their system, is quite limited in terms of the available bandwidth for the probe pulse. This is because the two fields responsible for the Raman gain cannot be too far detuned from resonance. The trade off between achieving sufficiently large gain so as to obtain sharp change in dispersion in between the gain lines, and having the gain lines separated far enough so as to obtain minimal gain at the line center severely restricts the bandwidth in their system. Moreover, Doppler broadening further reduces the desirable anomalous region. In most other schemes too one lacks the control over the separation between closely spaced doublet exhibiting inversion, as the doublets arise from either hyperfine splitting or isotope shift [26]. This limitation is overcome in our system because the bandwidth depends on the frequency of modulation and one can achieve a few hundred GHz modulation frequency at optical frequencies. Another advantage of this system is availability of multiple periodically separated gain peaks so that one could choose to operate the probe far off resonance and thus the possibility of decreasing the noise arising from spontaneous emission [27]. Hence, our system in principle accords more flexibility in obtaining anomalous dispersion region of desired frequency bandwidth in a desired frequency regime. The possibility of tailoring dispersion/absorption-gain characteristics by controlling different parameters of the modulation and the incoherent pump to overcome restrictions due to Doppler broadening and power broadening are added advantages of this system.

We now discuss in detail the resonant case where the central frequency of the FM field is on resonance with the  $|1\rangle \leftrightarrow |3\rangle$  transition and contrast our results with the traditional monochromatic ( $M = 0$ ) case. In the monochromatic pump case, gain arises purely from the coherence between the excited states  $|1\rangle$  and  $|2\rangle$  which are not dipole connected, and, has been shown to occur without inversion in any state basis [21]. We calculate the steady-state response of the system in presence of modulation and Fig. 5a depicts the gain obtained as a function of the index of modulation  $M$ . At  $M = 0$  one obtains the gain typical of the monochromatic case, whereas for strong modulation ( $M$  away from zero) one finds much larger gain. The  $\operatorname{Im}(\rho_{32})$  at  $M = 10.17$  is  $3.75 \times 10^{-5}$  in comparison to  $3.05 \times 10^{-6}$  at  $M = 0$ , a  $\sim 10^3\%$  increment over the monochromatic case. It should be borne in mind that the dynamics in presence of strong modulation is such that significant contributions occur from the numerous side-band resonances leading to such large gain.

The absorption peaks (sharp dips in Fig. 5a) occur at those values of  $M$  for which  $J_0(M) = 0$ , note that we have chosen  $\Omega \gg \gamma_1$ . This effect is expected on physical grounds as one can see from the spectral content of the FM field, namely

$$e^{iM \sin(\Omega t)} = \sum_{p=-\infty}^{+\infty} J_p(M) e^{ip\Omega t}, \quad (16)$$

where  $J_p(M)$  is the Bessel function of integer order  $p$ . Whenever the resonant central frequency is absent on the  $|1\rangle \leftrightarrow |3\rangle$  transition the population in level  $|3\rangle$  dominantly experiences absorption on the  $|3\rangle \leftrightarrow |2\rangle$  transition, and the large value of  $\Omega$  also ensures that spectral components at  $\pm\Omega$  with the weight of  $J_{\pm 1}(M)$  are far removed in frequency from the resonant line center. In between these peaks of absorption one obtains gain. The fact that one obtains gain only when  $J_0(M) \neq 0$  points toward the spontaneous emission assisted nonlinear optical process responsible for gain which will be discussed in detail at the end of this section.

In terms of the density matrix the major contribution to the gain is from the modulation term  $F_3$  of Eq. (6) as seen in Fig. 5b. For  $M = 0$  the contribution from the inversion term  $F_1$  is negative while the positive coherence term  $F_2$  completely offsets this and is responsible for gain. The  $F_3$  term is zero at  $M = 0$  and starts increasing as  $M$  gets larger. For strong modulation the  $F_3$  term largely overshadows all other contributions and is responsible for gain in between the zeros of  $J_0(M)$ . The smaller dips in the  $F_3$  component, that occur in between the the zeros of the  $J_0(M)$ , result from the next higher contribution arising from  $\omega_1 \pm \Omega$ . These set of dips that occur when  $F_3$  is large and positive are due to the zeros of the the Bessel  $J_1(M)$ . The weights of the contribution at  $\omega_1 \pm \Omega$  are  $J_{\pm 1}(M)$ , these contributions are absent when  $M$  takes values such that  $J_1(M) = 0$ . It should be noted that even though the contribution from  $\pm\Omega$  disappears at these values of  $M$ , the contribution from higher multiples of  $\Omega$  continues to be significant resulting in large  $F_3$  term and the resulting gain. The steady state population distribution is shown in Fig. 5c. At  $M = 0$ ,  $\rho_{22} < \rho_{11} < \rho_{33}$  and this results in gain without inversion in the bare state basis as well as no inversion for the Raman process. For  $M = 3.7$  where the gain is  $1.6 \times 10^{-5}$  about  $\sim 400\%$  more than the monochromatic case, the relative population distribution is the same, i.e.,  $\rho_{22} < \rho_{11} < \rho_{33}$ ; there is no inversion in the bare state basis as well as no inversion for the stimulated Raman scattering (SRS) process. The two photon SRS inversion condition requires that  $\rho_{22} > \rho_{11}$ . For very large values of  $M$ , not shown in figure, even though there is no inversion in the bare state basis ( $\rho_{22} < \rho_{33}$ ) there is Raman inversion for the SRS process namely the  $|2\rangle \rightarrow |3\rangle \rightarrow |1\rangle$  process, because  $\rho_{22}$

becomes larger than  $\rho_{11}$ . Note that in all our discussions the feature of the gain being inversionless is between the bare atomic states  $|1\rangle$ ,  $|2\rangle$  and  $|3\rangle$ .

## B. Transient dynamics

We discuss the time evolution of atomic polarization and population distribution in the FM field pumped V-type system and how it approaches the steady state values. Due to the presence of a strong FM field the transient response of the system is very complex making it difficult to identify the physical mechanism responsible for gain. We consider in detail one case in which one can identify the dominant process and is comparable to the monochromatic pump case. We will also present a general case wherein the dynamics is more complex.

We choose the on-resonance case where  $\Delta_1 = \Delta_2 = 0$ , the modulation frequency is large ( $\Omega = 80\gamma_1$ ) and the index of modulation is chosen such that it is a zero of the first order Bessel function, i.e.,  $J_1(M) = 0$  for  $M = 10.1734$ . This particular choice is such that the FM field spectrum has the central peak at  $\omega_1$  with weight  $J_0(M)$ , no peak at  $\omega_1 \pm \Omega$  as  $J_1(M) = 0$ , the next peak in frequency is far removed and is at  $\omega_1 \pm 2\Omega$  with weight  $J_2(M)$ , and other peaks at  $\omega_1 \pm n\Omega$  with  $n > 2$  and weight  $J_n(M)$  are further removed from resonance. Choice of large  $\Omega$  and the appropriate  $M$  ensures that the effects of  $\omega_1 \pm n\Omega$  for  $n \neq 0$  are minimal and the population and atomic polarization dynamics appear to be somewhat similar to the monochromatic pump case.

In Fig. 6a we show the evolution of the population in presence of the incoherent pump with the initial condition  $\rho_{33} = 1$  and all other  $\rho_{ij} = 0$  ( $i, j=1-3$ ). It is seen that at all times  $\rho_{22} < \rho_{33}$  and  $\rho_{22} < \rho_{11}$ , therefore, there is no population inversion in the bare state basis and there is no Raman inversion for gain through SRS process, respectively. Fig. 6b shows the evolution of population in absence of the incoherent pump. The population in level  $|2\rangle$  is negligible because the probability of the population to be excited to level  $|2\rangle$  is very small as  $G_2 \ll G_1$  and  $\gamma_i$ . As expected the population oscillates between level  $|1\rangle$  and  $|3\rangle$  and in steady state  $\rho_{11} \approx \rho_{33} \approx 0.5$ , though  $\rho_{33}$  is slightly larger than  $\rho_{11}$  due to the presence of the FM field and the decays. It is also observed that in presence of the incoherent pump the population and the atomic coherences reach their steady state values earlier in time. Fig. 6c(d) shows the evolution of gain-absorption for the probe field (FM pump field at  $\omega_1$ ) with and without the incoherent pump. We note the following: they both oscillate dominantly with the same frequency and nearly in phase with each other. Both the probe and the pump field experience gain in the transient regime with or without the incoherent pump. In presence of the incoherent pump only the probe field experiences gain in the steady state, whereas with  $\Lambda = 0$  both the fields experience absorption in the steady state.

The probe field experiences gain just after  $\rho_{33}$  reaches a minimum value favoring the stimulation process from  $|2\rangle \rightarrow |3\rangle$  rather than the  $|3\rangle \rightarrow |2\rangle$  transition. The probe field experiences gain in the interval when  $d\rho_{33}/dt > 0$  and reaches its maximum value at a time when  $d\rho_{33}/dt$  is the steepest. The FM pump field at the  $\omega_1$  frequency experiences gain just after  $\rho_{11}$  reaches its maximum value. The contribution to the envelop of the pump gain does not seem to come from SRS process even though the two-photon inversion with  $\rho_{11} > \rho_{22}$  is present. The signature for an SRS process would be that the absorption-gain response on the  $|1\rangle \leftrightarrow |3\rangle$  and  $|2\rangle \leftrightarrow |3\rangle$  transitions be out of phase. In other words, emission on one transition accompanied by absorption on the other transition. This is however not present in this case as the envelopes oscillate in phase with each other as seen in Figs. 6c and d. We re-emphasize that the gain in the above parameter regime is qualitatively akin to the monochromatic case apart from the rapid but weak (small amplitude) oscillations due to the FM field on the central pump frequency  $\omega_1$  in Fig. 6d.

We present in Fig. 7 the temporal evolution of the atomic polarization and the population dynamics when the central frequency of the FM field is detuned from the atomic resonance. The parameters chosen are identical to that in Fig. 2 which corresponds to the steady state behavior. The population initially is in level  $|3\rangle$ . The probe frequency is tuned to the gain peak at  $\Delta_2 = 46.8\gamma_1$ . We observe that the population in levels  $|1\rangle$  and  $|3\rangle$  oscillate  $\sim 180^\circ$  out of phase with respect to each other. The population in  $|2\rangle$  is negligible in absence of the incoherent pump and steadily increases in presence of the incoherent pump, see Figs. 7a-b. At time  $\tau\gamma_1 \approx 3$  the population  $\rho_{22}$  becomes larger than the population  $\rho_{11}$ , however,  $\rho_{22}$  remains smaller than  $\rho_{33}$  at all times. Again there is no population inversion between the levels  $|2\rangle$  and  $|3\rangle$ . After time  $\tau\gamma_1 \approx 3$ , unlike the resonant case shown in Fig. 6, the population  $\rho_{22} > \rho_{11}$  implying inversion for the SRS process for probe gain.

Both the probe and the pump fields experience gain in the transient region with or without the incoherent pump. It is clear that gain on the central FM frequency  $\omega_1$  results just after  $\rho_{11}$  reaches its maximum value. Apart from the high frequency oscillations the envelop of the polarization on the central FM frequency  $\omega_1$  closely follows the  $\rho_{11}$  oscillations. These high frequency oscillations riding on the envelop result from higher order contributions of field at  $\omega_1 \pm n\Omega$  for  $n > 0$ . There is no gain in the steady state at the  $\omega_1$  frequency, whereas the probe field experiences gain in the steady state.

The frequency of oscillation of the probe field depends on its generalized Rabi frequency and is found to be

independent of the incoherent decays and the incoherent pump. A closer look at the probe oscillations in Fig. 7c shows that periodically there are larger peaks of gain which invariably follow just after  $\rho_{33}$  reaches a minimum value, pointing to similar process discussed above. Moreover, due to the complexity of the time evolution one cannot rule out SRS process as some peaks of probe gain do match with pump absorption dips and vice-versa.

### C. Physical mechanism for gain

Although the quantitative results obtained above from solving the density matrix equations provide complete description of the system under consideration, it still does not provide insight into the underlying nonlinear optical processes. Deeper understanding can be obtained by systematically summing up individual scattering processes and identifying the dominant contributions to the gain. We have observed that in the steady state the probe gain occurs only if  $\gamma_1 > \gamma_2$  [28], implying that spontaneous emission plays a crucial role in obtaining inversionless gain [29]. In recent times irreversible spontaneous emission assisted nonlinear optical processes have been suggested which contribute to inversionless gain (in ladder-type systems by Sellin *et al* [30] and in  $\Lambda$ -type systems by Zhu [31]). Along these lines the physical picture for inversionless gain in the steady state for the V-type system would be the following. First a stimulated emission process from  $|2\rangle \rightarrow |3\rangle$  of the probe photon  $\omega_2$ , followed by absorption from  $|3\rangle \rightarrow |1\rangle$  and finally spontaneous emission from  $|1\rangle \rightarrow |3\rangle$  at the rate of  $2\gamma_1$ , see Fig. 8a. Note that the probe experiences significant stimulated emission only at certain frequencies due to the FM pump field, namely  $\omega_2 \pm n\Omega$ . These resonant features are absent in the conventional LWI schemes. It should also be noted that in the above process the second step involving absorption from  $|3\rangle \rightarrow |1\rangle$  depends critically on the availability of the  $\omega_1$  photon (for  $\Delta_1 = 0$ ). In its absence, when the index of modulation  $M$  is such that  $J_0(M) = 0$ , this nonlinear process is suppressed and the probe experiences only absorption, see Fig. 5a. The competing process (Fig. 8b), of stimulated emission from  $|1\rangle \rightarrow |3\rangle$  followed by absorption from  $|3\rangle \rightarrow |2\rangle$  and spontaneous emission from  $|2\rangle \rightarrow |3\rangle$  at  $2\gamma_2$  rate, is less preferred because of  $\gamma_1 > \gamma_2$ . Thus the former process plays a dominant role in inversionless probe gain.

We have described above the nonlinear optical process responsible for gain when the central FM frequency  $\omega_1$  is resonant with the atomic transition. We have also looked at detuned cases and similar nonlinear process seems to form the basis for obtaining gain. We describe briefly one such detuned case, wherein  $\Delta_1$  is finite and  $\Omega$  is chosen to be equal to  $\Delta_1$ . It is clear that, in this case, the  $\omega_1 + \Omega$  photon would be required in the second step of the nonlinear process (Fig. 8a) instead of the  $\omega_1$  photon. This is further supported by looking at the polarization  $\text{Im}(\rho_{32})$  as a function of  $M$ , and one observes sharp absorption at those values of  $M$  for which  $J_1(M) = 0$  (not shown here). This clearly shows that in absence of the  $\omega_1 + \Omega$  photon there would be no spontaneous emission assisted gain process. Hence, the availability of the intermediate photon which would take the population from level  $|3\rangle$  to level  $|1\rangle$  and the probe resonant with the periodic sideband response created by the FM field plays a crucial role in obtaining large gain.

It should be noted that the nonlinear optical process discussed above is *assisted* by the spontaneous emission and hence does not necessitate any kind of population inversion. The FM field plays a central role in creating the rich periodic Floquet structure whose quasienergy levels are probed by the probe field. The on-resonance pump photon acts as a hub about which the above nonlinear process occurs resulting in gain. We would also like to point out that if an amplitude modulated field (with modulation frequency  $\alpha$ ) is used instead of the FM field, then, due to the availability of only a pair of sideband photons ( $\omega_1 \pm \alpha$ ) the gain from the above nonlinear process will be present only at a pair of frequencies. It is the availability of  $\omega_1 \pm n\Omega$  photons in the FM field that results in gain at a large number of sideband frequencies far removed from the central frequency.

## IV. CONCLUSION

In summary, we have presented an analysis of the occurrence of gain in a V-type system in presence of FM pump field. We have analyzed both the steady state and the transient dynamics of the light amplification process. In the steady state analysis we have tried to bring out the significant role played by the modulation term over and above the coherence term which is dominant in the conventional monochromatic pump schemes. We obtained the Floquet quasienergies that provide the explanation for the two comb of frequencies in the probe spectrum; furthermore the quasienergy spectrum was used to choose appropriate index of modulation  $M$  such that the resulting probe spectrum contains a semi-infinite set of consecutive gain peaks far removed from resonance and could be exploited to obtain short-wavelength lasing. In between the gain peaks anomalous dispersion is obtained accompanied by negligible gain-absorption, which could be utilized to obtain distortion free superluminal pulse propagation in any desired frequency regime and over a large bandwidth which can be increased by increasing the modulation frequency  $\Omega$ . The gain



obtained in experiments based on LWI schemes is severely limited in its magnitude. The advantage of gain obtained using the FM field is the significant increment in its magnitude  $\sim 10^3\%$  due to numerous sideband contributions, and no population inversion between the atomic states. It should be noted that the occurrence of gain at frequencies far removed from resonance could also make this system attractive in terms of the possibility of reduced noise due to quantum fluctuations, further investigations along these lines would be fruitful. The study of transient dynamics showed that both the probe and the pump fields experience transient gain. The probe gain is not due to population inversion in the atomic state basis, moreover, in certain regimes one could even rule out gain via SRS process and two-photon inversion. We have described the physical process, based on spontaneous emission assisted nonlinear optical process, which is responsible for inversionless gain. This effect is further corroborated by the spectrum obtained as a function of the index of modulation in Fig. 5a.

- 
- [1] For reviews see E. Arimondo, in *Progress in Optics XXXV* edited by E. Wolf (Elsevier Science, Amsterdam, 1996), p. 257; S.E. Harris, Phys. Today **50** 36 (1997); M.O. Scully and M.S. Zubairy, *Quantum Optics* (Cambridge University Press, Cambridge, England 1997), Chaps. 7 and 14.
- [2] O. Kocharovskaya, Phys. Rep. **219**, 175 (1992); M.O. Scully, *ibid* **219**, 191 (1992); P. Mandel, Contemp. Phys. **34**, 235 (1993); J. Mompert and R. Coribalán, J. Opt. B: Quant. Semicl. Opt. **2**, R7 (2000).
- [3] A. Nottelmann, C. Peters, and W. Lange, Phys. Rev. Lett. **70**, 1783 (1993); E. S. Fry, X. Li, D. Nikonov, G. G. Padmabandu, M. O. Scully, A. V. Smith, F. K. Tittel, C. Wang, S. R. Wilkinson, and S.-Y. Zhu, *ibid* **70**, 3235 (1993); W. E. van der Veer, R. J. J. van Diest, A. Dönszelmann, and H. B. van Linden van den Heuvell, *ibid* **70**, 3243 (1993).
- [4] Y. Zhu and J. Lin, Phys. Rev. A **53**, 1767 (1996); Y. Zhu, J. Lin, and P. Sanchez, Opt. Commun. **128**, 254 (1996); J. A. Kleinfeld and A. D. Streater, Phys. Rev. A **53**, 1839 (1996); C. Fort, F. S. Cataliotti, T. W. Hänsch, M. Inguscio, and M. Prevedelli, Opt. Commun. **139**, 31 (1997).
- [5] A. S. Zibrov, M. D. Lukin, D. E. Nikonov, L. Hollberg, M. O. Scully, V. L. Velichansky, and H. G. Robinson, Phys. Rev. Lett. **75**, 1499 (1995); G. G. Padmabandu, G. R. Welch, I. N. Shubin, E. S. Fry, D. E. Nikonov, M. D. Lukin, and M. O. Scully, *ibid* **76**, 2053 (1996); F. B. de Jong, A. Mavromanolakis, R. J. C. Spreeuw, and H. B. van Linden van den Heuvell, Phys. Rev. A **57**, 4869 (1998).
- [6] A. E. Kaplan, Zh. ksp. Teor. Fiz. **68**, 823 (1975) [Sov. Phys. JETP **41**, 409 (1976)].
- [7] L. Hall, L. Hollberg, T. Baer and H. G. Robinson, Appl. Phys. Lett. **39**, 680 (1981); J. H. Shirley, Opt. Lett. **7**, 537 (1982).
- [8] G. S. Agarwal, Phys. Rev. A **23**, 1375 (1981).
- [9] G.C. Bjorklund, Opt. Lett. **5**, 15 (1980); G.C. Bjorklund and M. D. Levenson, Phys. Rev. A **24**, 166 (1981); G.C. Bjorklund, M. D. Levenson, W. Lenth and C. Oritz, Appl. Phys. B **32**, 145 (1983).
- [10] N. Nayak and G.S. Agarwal, Phys. Rev. A **31**, 3175 (1985).
- [11] J. A. Silver, Appl. Opt. **31**, 707 (1992); H. Ririos, C. B. Carlisle, R. E. Warren and D. E. Cooper, Opt. Lett. **19**, 144 (1994).
- [12] W. M. Ruyten, Phys. Rev. A **42**, 4226 (1990).
- [13] M. Janowicz, Phys. Rev. A **44**, 3144 (1991).
- [14] A. V. Alekseev and N. V. Sushilov, Phys. Rev. A **46**, 351 (1992).
- [15] G. S. Agarwal and W. Harshawardhan, Phys. Rev. A **50**, R4465 (1994).
- [16] V.N. Smelyanskiy, G.W. Ford and R.S. Conti, Phys. Rev. A **53**, 2598 (1996); V.N. Smelyanskiy, R.S. Conti and G.W. Ford, Phys. Rev. A **55**, 2186 (1997).
- [17] W. Harshawardhan and G.S. Agarwal, Phys. Rev. A **55**, 2165 (1997).
- [18] Y. Zhu, A. Lezama, D.J. Gauthier and T. Mossberg, Phys. Rev. A **41**, 6574 (1990); H.S. Freedhoff and Z. Chen, Phys. Rev. A **41**, 6013 (1990); **46**, 7328(E) (1992); G.S. Agarwal, Y. Zhu, D. J. Gauthier and T. Mossberg, J. Opt. Soc. Am. B **8**, 1163 (1991).
- [19] M.F. Van Leeuwen, S. Papademetriou, and C.R. Stroud, Jr., Phys. Rev. A **53**, 990 (1996); S. Papademetriou, M.F. Van Leeuwen, and C.R. Stroud, Jr., Phys. Rev. A **53**, 997 (1996).
- [20] D. Goswami and W.S. Warren, Phys. Rev. A **50**, 5190 (1994).
- [21] Y. Zhu, Phys. Rev. A **45**, R6149 (1992); Y. Zhu, *ibid* **53**, 2742 (1996).
- [22] G.S. Agarwal, Phys. Rev. A **44**, R28-R30 (1991).
- [23] L.J. Wang, A. Kuzmich and A. Dogariu, Nature **406**, 277 (2000); A. Dogariu, A. Kuzmich and L.J. Wang, Phys. Rev. A **63** 053806 (2001).
- [24] H. Risken, *The Fokker-Planck Equation* (Springer-Verlag, Berlin, 1984), p. 196.
- [25] J.H. Shirley, Phys. Rev. **138** B 979 (1965).
- [26] A.M. Steinberg and R.Y. Chiao, Phys. Rev. A **49**, 2071 (1994); R.Y. Chiao, Phys. Rev. A **48**, R34 (1993).
- [27] A. Kuzmich, A. Dogariu, L.J. Wang, P.W. Milonni and R.Y. Chiao, Phys. Rev. Lett. **86**, 3925 (2001).
- [28] The ratio  $\gamma_2/\gamma_1$  is chosen to be much smaller than unity in Figs. 2 and 3 to highlight the two comb of resonances resulting from the two linearly independent set of solutions of the Floquet Hamiltonian (11). The necessary condition for obtaining steady state probe gain is  $\gamma_2 < \gamma_1$ .
- [29] P.B. Sellin, C.C. Yu, J.R. Bochinski, and T.W. Mossberg Phys. Rev. Lett. **78**, 1432 (1997).
- [30] P.B. Sellin, G.A. Wilson, K.K. Meduri and T.W. Mossberg, Phys. Rev. A **54**, 2402 (1996).
- [31] Y. Zhu, Phys. Rev. A **55**, 4568 (1997).

## Figure Captions

FIG. 1. Schematic of the V-type system coupled to a frequency modulated field on the  $|1\rangle \leftrightarrow |3\rangle$  transition, the central frequency  $\omega_1$  of the FM field is shown with a dash-dot line. A monochromatic probe field of frequency  $\omega_2$  and an incoherent pump  $\Lambda$  (dotted line) couple the  $|2\rangle \rightarrow |3\rangle$  transition. The spontaneous emission decays from levels  $|1\rangle$  and  $|2\rangle$  to level  $|3\rangle$  are represented by  $\gamma_1$  and  $\gamma_2$  (wavy line), respectively. The detuning of the central frequency  $\omega_1$  of the FM field from the atomic resonance is  $\Delta_1$  and the probe detuning is  $\Delta_2$ .

FIG. 2. Steady state probe absorption-gain spectra - (a) Without the incoherent pump the probe exhibits absorption as  $\text{Im}(\rho_{32}) < 0$ . (b) In presence of the incoherent pump with  $\Lambda = 0.1\gamma_1$  alternate peaks exhibit gain. (c) The contribution to  $\rho_{32}$  from the terms  $F_1$  and  $F_2$  is significant only at frequencies given by Eq. (7), whereas the contribution from the modulation term  $F_3$  is the largest. The other relevant parameters are  $M = 5.2$ ,  $\Omega = 30\gamma_1$ ,  $\Delta_1 = 20\gamma_1$ ,  $G_1 = 20\gamma_1$ ,  $G_2 = .01\gamma_1$ , and  $\gamma_2 = 0.03\gamma_1$ . The scale on the graphs is chosen to highlight the sideband structure and hence some of the maxima of the resonances are not shown.

FIG. 3. (a) Plot of a few quasienergies  $\lambda$  vs  $M$  for a fixed value of coupling field strength  $G_1 (= 20\gamma_1)$ , detuning  $\Delta_1 (= 20\gamma_1)$  and the modulation frequency  $\Omega (= 30\gamma_1)$ . The quasienergy level indicated by a solid line periodically crosses the zero energy level. (b) Steady state probe response for various values of  $\Lambda$  with the index of modulation  $M = 2.915$  which is the first zero of the quasienergy level shown in (a) by a solid line. The line plots are for incoherent pump  $\Lambda/\gamma_1 = 0, 0.2, 0.4, 0.6, 0.8$  and  $1.0$ . The other relevant parameters are  $G_2 = .01\gamma_1$ , and  $\gamma_2 = 0.03\gamma_1$ . The scale on the graphs is chosen to highlight the sideband structure and hence some of the maxima of the resonances are not shown.

FIG. 4. Enlarged plot of the atomic response in the region  $\Delta_2/\gamma_1 = (70, 120)$  with all the parameters same as Fig. 3 and  $M = 2.915$ . In the region  $\Delta_2/\gamma_1 = (90, 100)$  the probe field experiences anomalous dispersion [ $d \text{Re}(\rho_{32})/d\omega_2 < 0$ ] accompanied by negligible absorption/gain [ $\text{Im}(\rho_{32}) \approx 0$ ]. Such regions occur between each pair of gain peaks for  $\Delta_2/\gamma_1 > 0$  in Fig. 3c. The slope of the  $\text{Re}(\rho_{32})$  can be further increased by increasing the rate of the incoherent pump.

FIG. 5. Plot of the resonant ( $\Delta_1 = \Delta_2 = 0$ ) steady state atomic response at the  $|3\rangle \leftrightarrow |2\rangle$  transition as a function of the index of Modulation  $M$ . (a) Absorption-gain at the probe transition, for  $M = 0$   $\text{Im}(\rho_{32}) = +3.05 \times 10^{-6}$  which is not clearly visible on the scale. (b) The individual contributions  $F_1, F_2$ , and  $F_3$  denoted by the dotted, dashed, and solid line, respectively. The  $F_2$  contribution is responsible for gain for weak modulation  $0 \leq M < 1$ ; for strong modulation  $F_3$  is the dominant term. To highlight the role played by the  $F_3$  term in obtaining gain the large absorption minima are not shown completely. (c) The population in various atomic levels: the solid, dashed and the dotted lines indicate  $\rho_{11}$ ,  $\rho_{22}$ , and  $\rho_{33}$ , respectively. The other relevant parameters are  $\Omega = 80\gamma_1$ ,  $G_1 = 20\gamma_1$ ,  $G_2 = .01\gamma_1$ ,  $\gamma_2 = 0.3\gamma_1$  and  $\Lambda = 0.5\gamma_1$ .

FIG. 6. Calculated transient atomic response for the same parameters as in Fig. 5 with the index of modulation  $M = 10.1734$  chosen to be a zero of the Bessel  $J_1(M)$  function. (a) Population distribution in presence of the incoherent pump ( $\Lambda = 0.5\gamma_1$ ). (b) Population distribution in absence of the incoherent pump ( $\Lambda = 0$ ). (c) Transient absorption-gain response at the probe frequency with and without the incoherent pump. (d) Transient absorption-gain response at the central frequency  $\omega_1$  of the FM field with and without the incoherent pump. All the atomic variables are plotted against normalized time  $\tau\gamma_1$ .

FIG. 7. Calculated transient atomic response for the same parameters as in Fig. 2 at the probe detuning  $\Delta_2 = 46.8\gamma_1$ . (a) Population distribution in presence of the incoherent pump ( $\Lambda = 0.1\gamma_1$ ). (b) Population distribution in absence of the incoherent pump ( $\Lambda = 0$ ). (c) Transient absorption-gain response at the probe frequency with and without the incoherent pump. (d) Transient absorption-gain response at the central frequency  $\omega_1$  of the FM field with and without the incoherent pump. All the atomic variables are plotted against normalized time  $\tau\gamma_1$ .

FIG. 8. The physical mechanism, involving spontaneous emission assisted nonlinear optical processes, responsible for inversionless gain. In steady state, process (a) prevails over process (b) because  $\gamma_1 > \gamma_2$ . Note also that when  $\Delta_1 = 0$ , for process (a) to occur the photon  $\omega_1$  has to be resonant with the  $|1\rangle \leftrightarrow |3\rangle$  transition. In its absence process (a) is suppressed resulting in probe absorption rather than probe gain.

Fig. 1

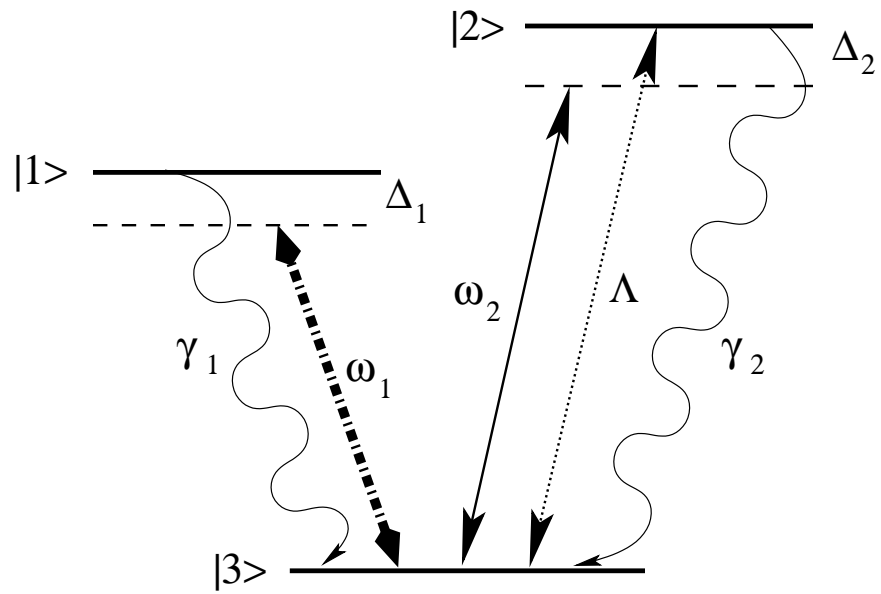


Fig. 2

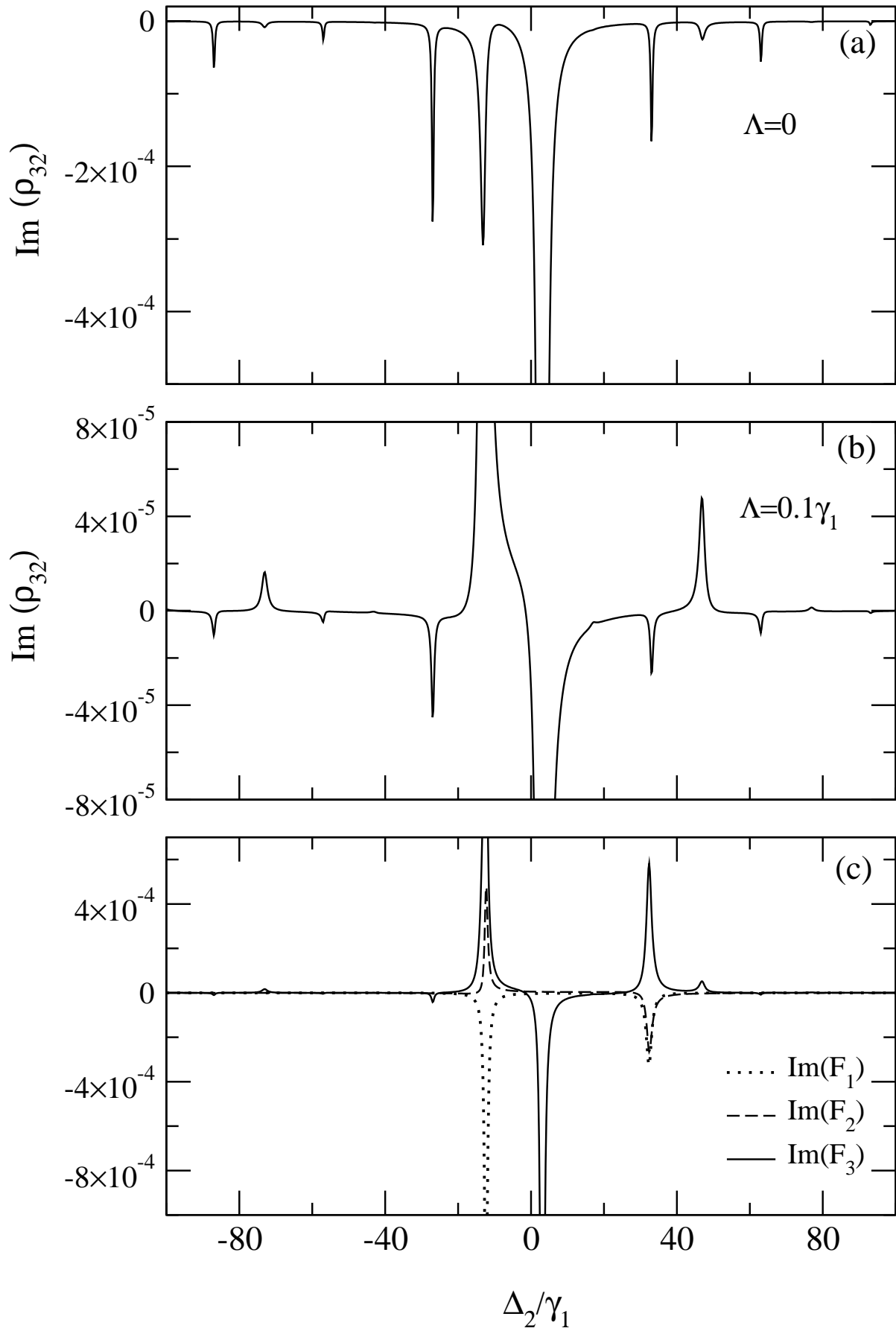


Fig. 3(a)

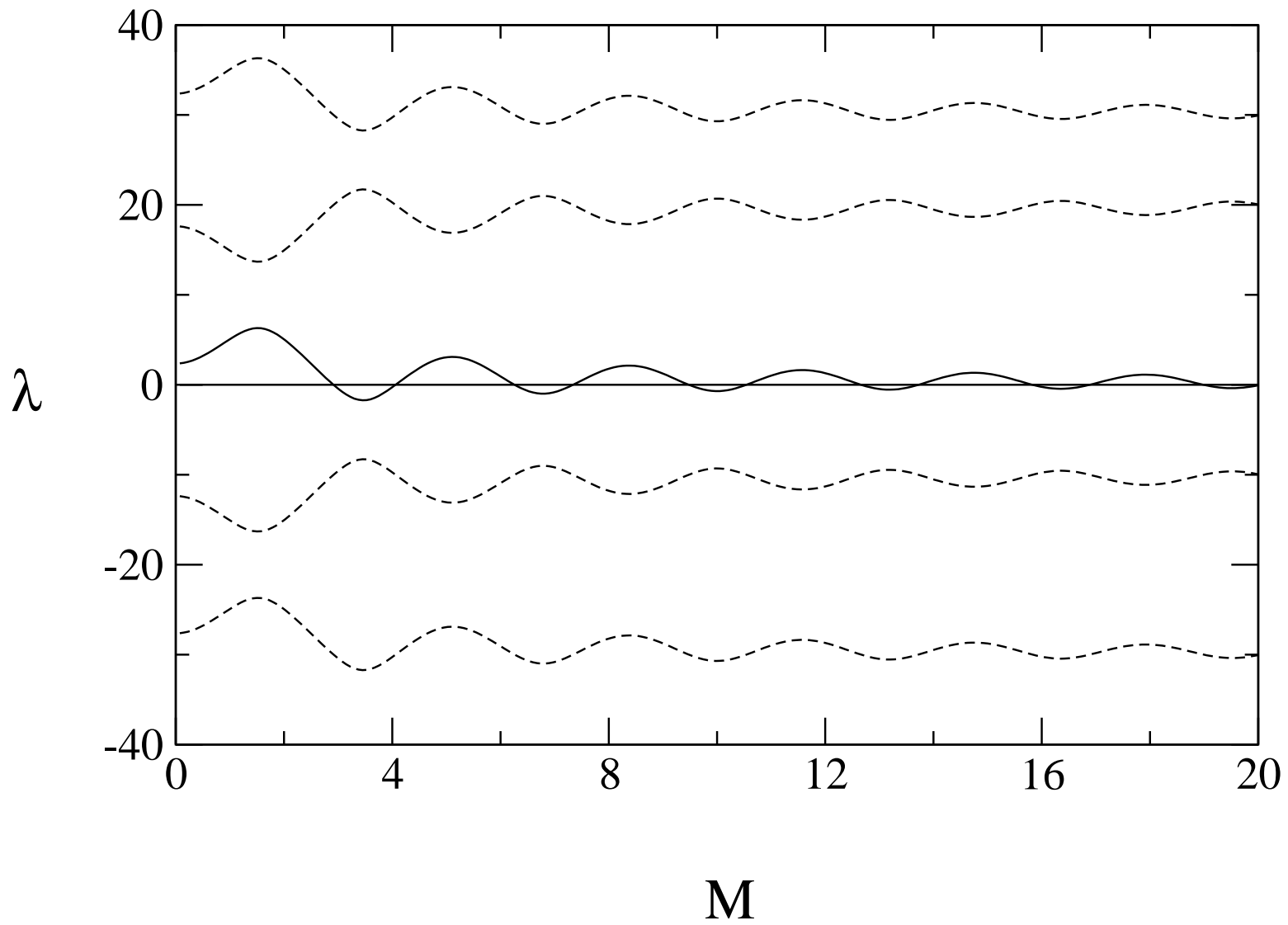


Fig. 3(b)

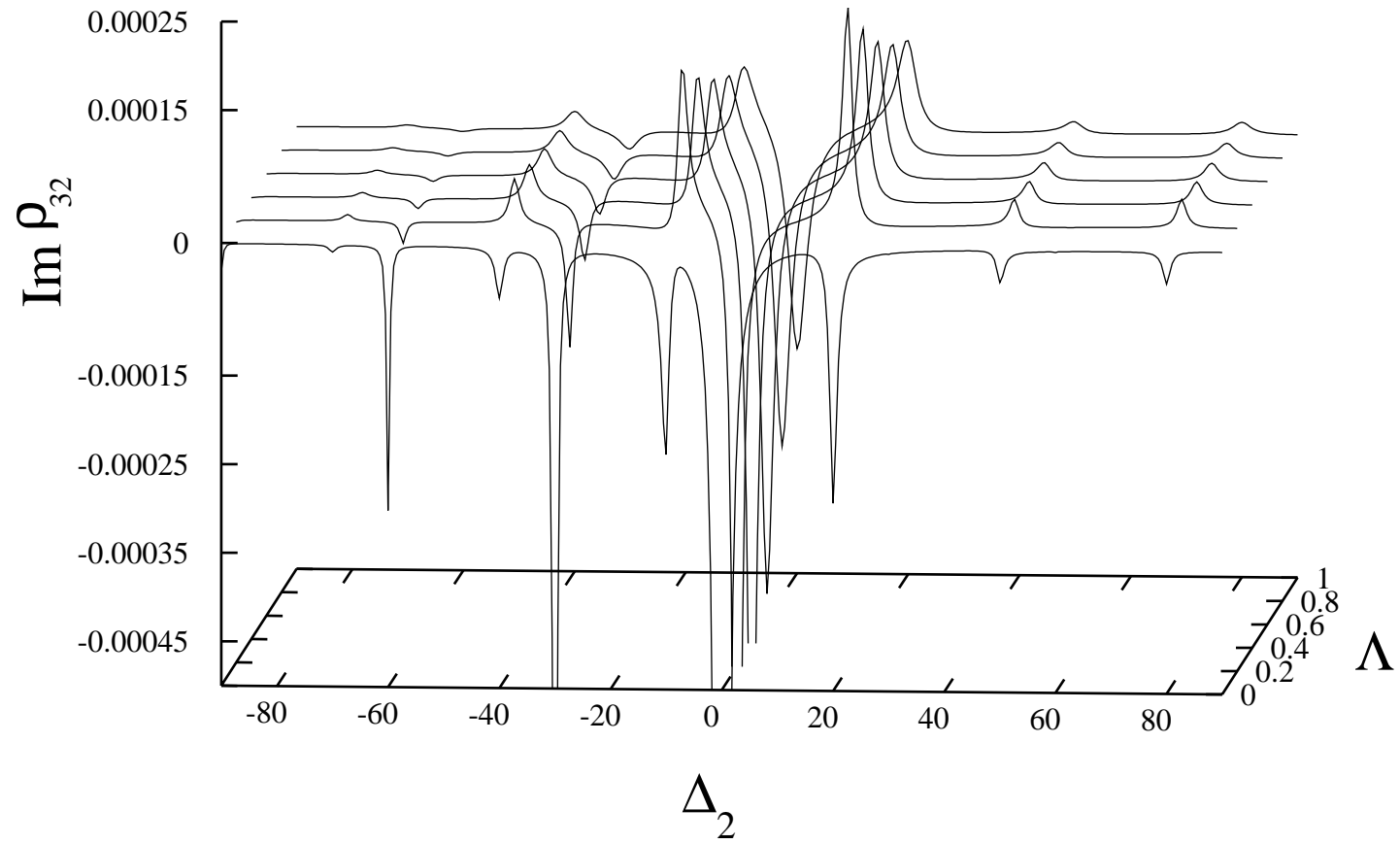


Fig. 4

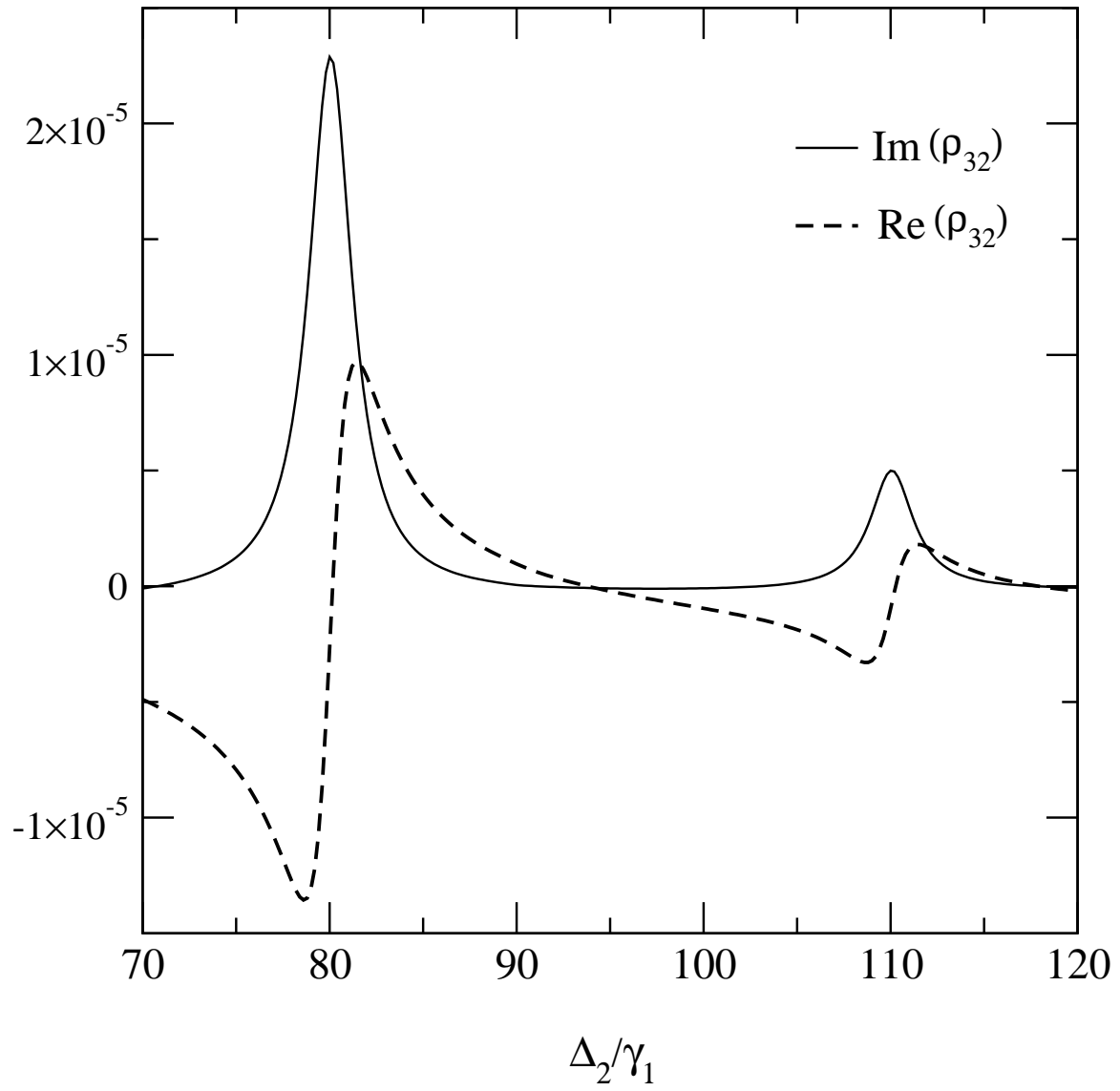




Fig. 5

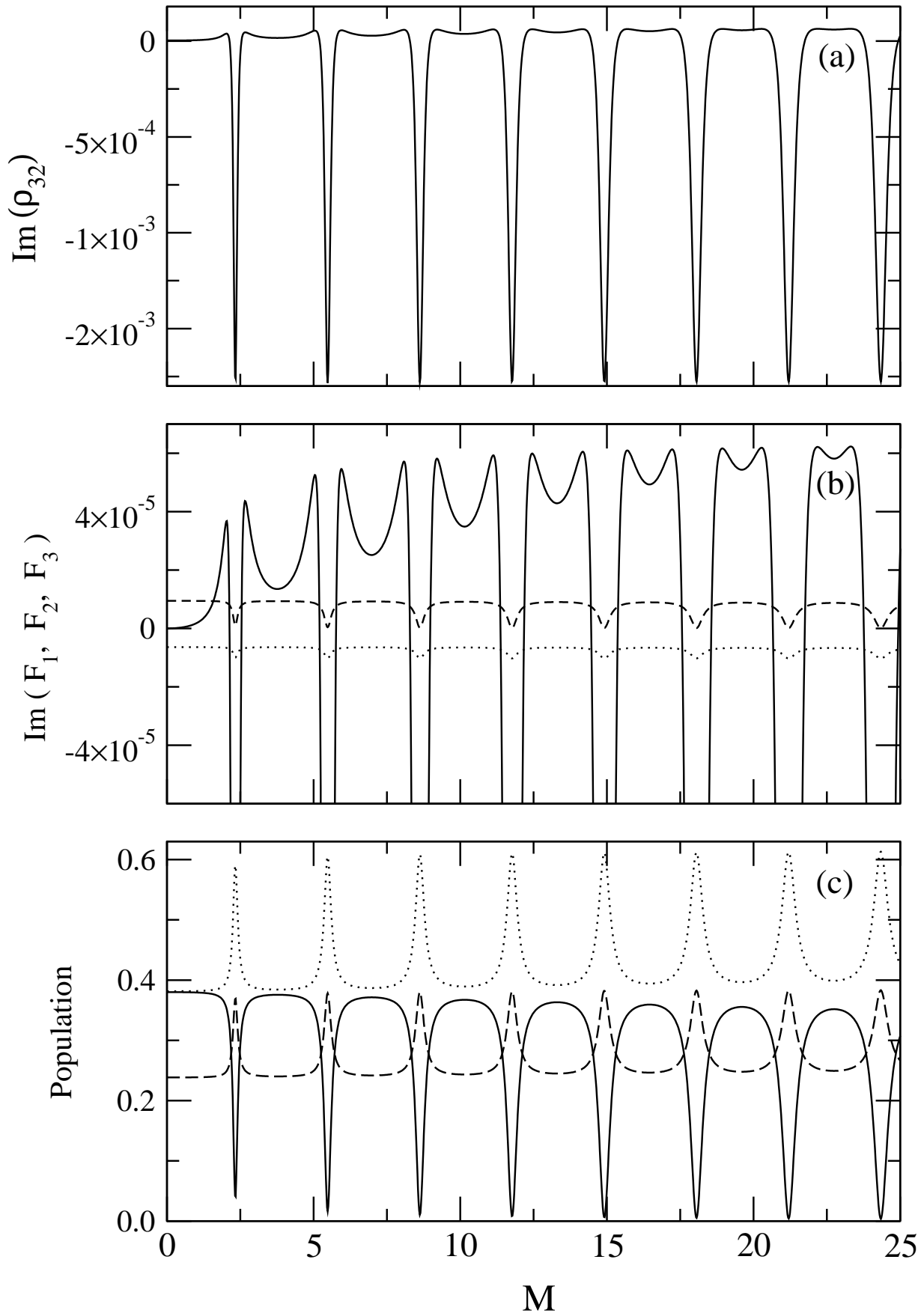


Fig. 6

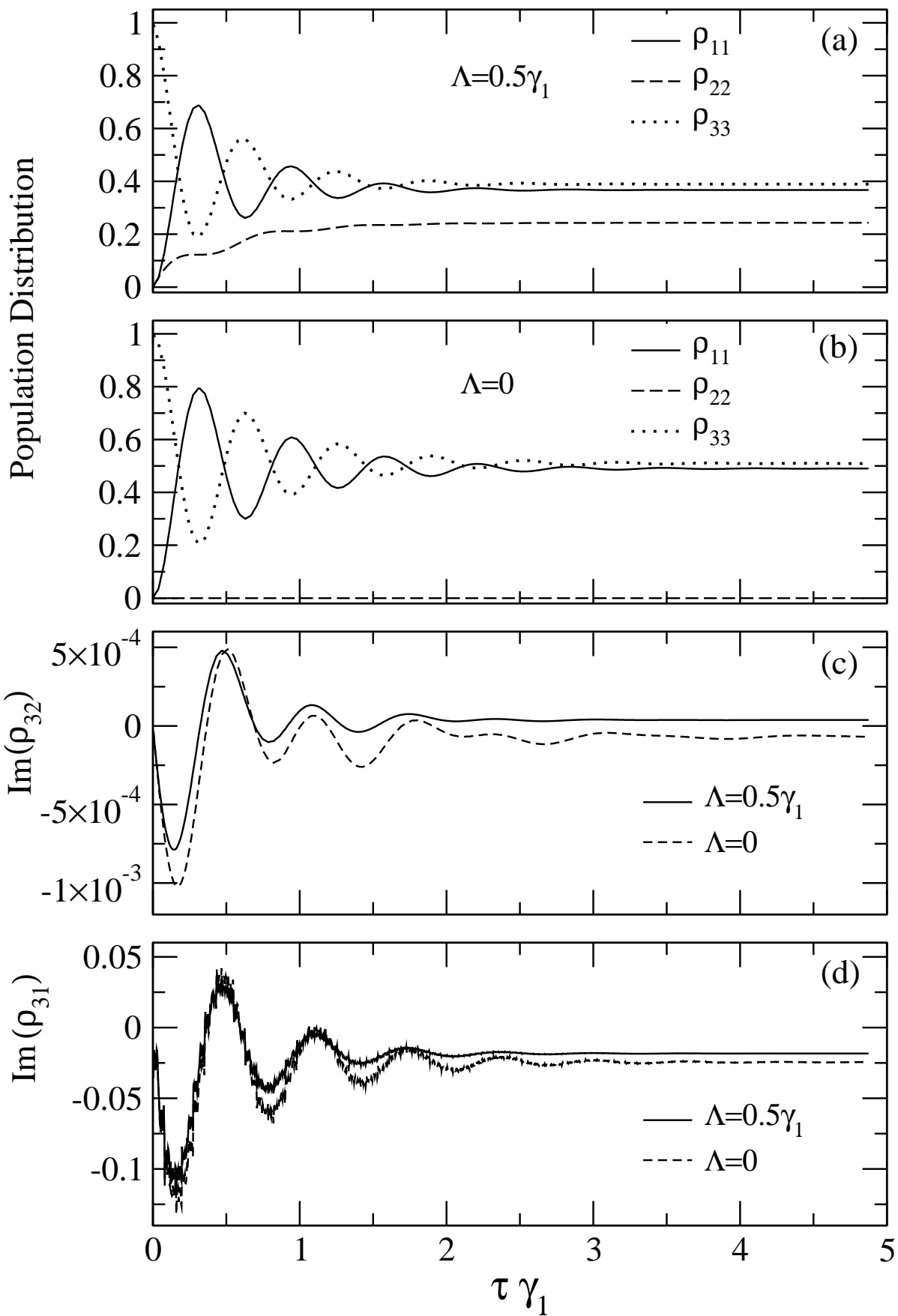


Fig. 7

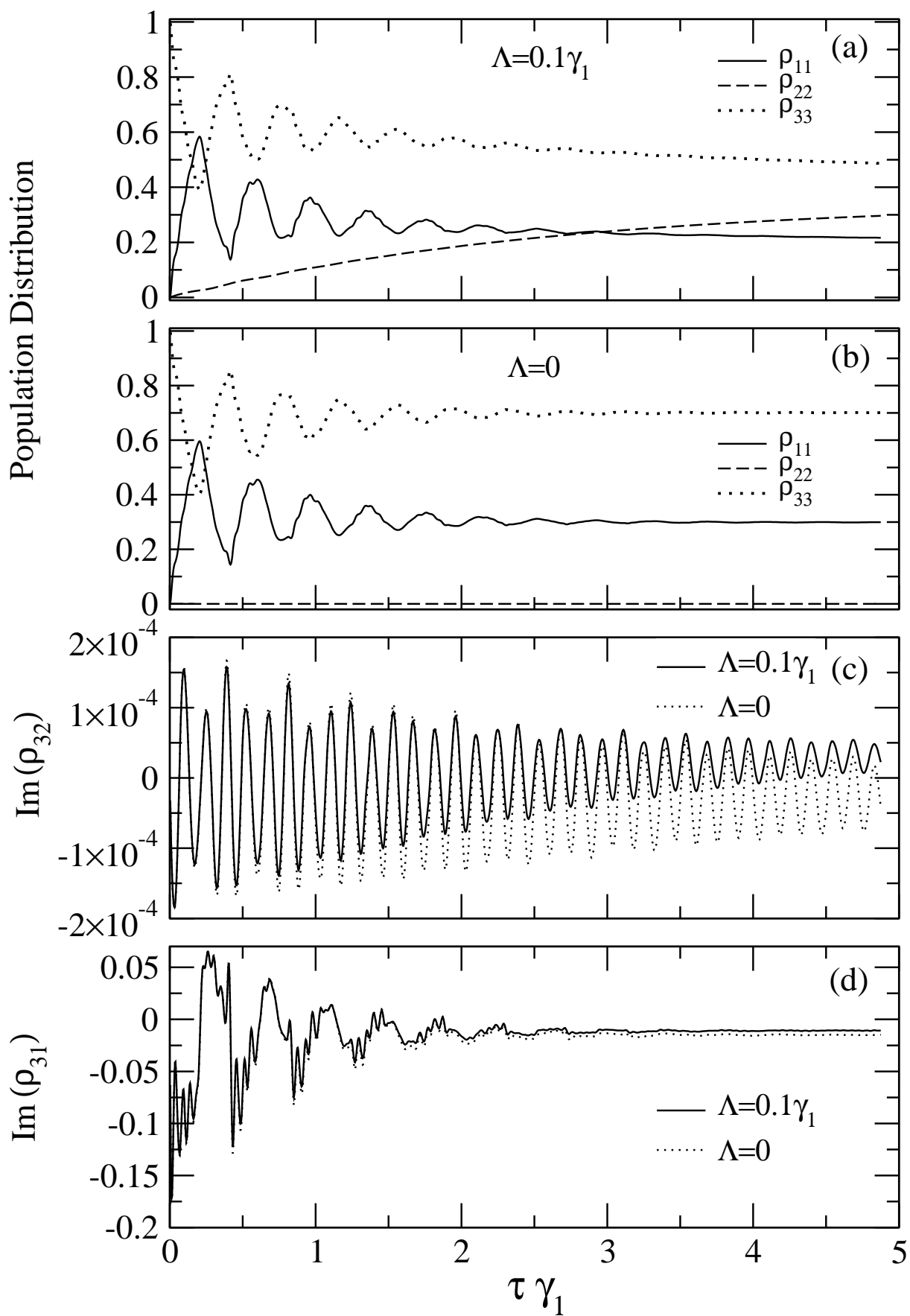


Fig. 8

